A Fluid Structure Interaction Model for Hydraulic Fracture Simulation on Vaca Muerta Argentina Shale Formation

I. D. Alderete, A. Sosa-Massaro, and S. D'Hers, Instituto Tecnológico de Buenos Aires

Abstract

Vaca Muerta Formation in Neuquén Basin, Argentina, is one of the great worldwide promises given its potential as a non-conventional reservoir. Because of the intrinsic heterogeneity and low permeability, hydraulic fracturing is a required operation to stimulate the reservoir for better production. Simulation becomes a desirable tool to make fractures more efficient and get predictable outcomes. For this purpose, a 3D finite element analysis is performed using ADINA software to model reservoir response during the hydraulic fracturing process.

This iterative, fully coupled model uses fluid structure interaction (FSI), porous elastic media and stratified materials with transversely isotropic (TI) properties. The allowed fracture distribution is proposed beforehand. A cohesive model is added via non linear springs placed along the fracture proposed path. Material models are calibrated using data from well logs and microseismics taken from one well located in the field. All the information obtained from that well is then filtered for a particular region of interest in depth, determined by the mechanical properties observed.

Regarding the calculation procedure, as initial condition for the stimulated reservoir volume (SRV) the stress strain state measured in the field is adopted. Then hydraulic fracture process is simulated pumping fluid through punched holes and then fracture opening is analyzed, based on nodes displacement along the proposed path, to characterize fracture's opening and extension. The resulting state of stress developed after the fracture is updated at every calculation step. Key information such as resulting pore pressure and effective stresses can be easily computed along the fracturing process.

Once obtained results are compared to analytical solutions and experimental data obtained from fractures performed in similar soil conditions with good agreement. The developed model can tackle a variety of reservoir volumes, considering stratification, geomechanical properties, fracture fluid, fracture paths and the initial state of stress. Natural cracks can be added in a rather simple fashion by adding fractures to the proposed distribution with adequate fracture strengths.

Introduction

Fracturing formations can be an excellent practise to increase production by creating a conductive path from the reservoir to the well. This procedure can be useful for conventional reservoir and also for non

conventional, given that, for example, by fracturing it is possible to increase the formation permeability allowing a new path connecting isolated pores containing production fluids. In the case of unconventional reservoirs with very low permeability (less than 0,001 md), hydraulic fracture can offer solutions, if correctly applied, to enhance production.

However, fracturing can be one of the most complex procedures performed on a well [1], not only for safety matters (high pressure, large volume of fluid and proppant injected, etc) and for the equipment required but also because a very high amount of variables that make the designing process extremely complex. Due to the high complexity of the process and the number of unknown variables involved, the outcome may not be the most desirable for completion engineers.

Hydraulic fracture from a strictly mechanical point of view is a procedure concerning four disciplines: continuum mechanics, fluid mechanics, fracture mechanics and mass transport. Coupling these disciplines in one 3D numerical model with the ability to predict the outcome, is a very desire tool, but quite challenging and a matter of huge interest for researchers.

The relatively recent capability for oil and gas industries to exploit unconventional reservoirs in an economically profitable way by using hydraulic fracture stimulations, has develop a growing interest in shale formation such as Vaca Muerta in Argentina, whose natural conditions were a constrain for production forecasting and stimulation design. Nowadays Vaca Muerta is great interest in the region and it is considered the second

Even though hydraulic fracture stimulation has been used since the 60's, process design is still challenging. Numerous hydraulic fracture models such as PKN (Perkins & Kern, 1961; Nordgren, 1972), KGD (Khristianovic, 1955; Geertsma & de Klerk, 1969) have been developed but they solutions are not always applicable since the great amount of different conditions one may encounter in the field. In addition, pseudo 3D (and even full 3D), are available, however not so widely accepted as the previously mentioned ones. Simulation of unconventional reservoirs is not a simple task due to inaccuracy in the geophysical model and the computational effort required to perform the calculations. This paper tackles the solution of a flow driven fracture in a poroelastic media taking into consideration the rock anisotropy by using real well information based on sonic logs, willing to explore shale behavior under such circumstances

Method

Models were developed using a Finite Element Analysis (FEA) software (ADINA, 2016). The software is chosen for its capability on Fluid-Structure Interaction problem solving. In order to use the fluid structure interaction feature, solid and fluid models must be developed separately and then boundary conditions in which the models will interact specified. Fracture path is defined in the mesh where cohesive material will be present. Material without cohesive interface defined cannot crack. This means that the initial fracture is already filled with fracturing fluid but with a closed section. Model evolves while fluid is pumped thus opening the crack until the final geometry of the fracture is obtainted. In addition to fracture geometry, resultant stresses and pore pressure's evolution during pumping is computed to follow stress changes along the process.

The fluid structure interaction formulation implies compatibility between the kinematic and dynamic conditions at the fluid structure boundary. This means,

$$\underline{d}_{fluid} = \underline{d}_{structure},\ displacement\ compatibility \tag{1}$$

$$\boldsymbol{n} \cdot \underline{\tau}_{fluid} = \boldsymbol{n} \cdot \underline{\tau}_{structure},\ traction\ equilibrium \tag{2}$$

Where d stands for the displacement fields and $\underline{\tau}$ stands for stress.

For this particular problem, a two-way, iterative coupling analysis strategy is addopted. Force and displacement criteria is adopted to check for iteration convergence. Iterative FSI coupling implies that the

fluid and solid equations are solved individually and successively, using the latest information provided by one of the models to feed the other of the coupled system. Iteration process continues until convergence criteria is reached in both solid and fluid models.

For describing rock's material anisotropic properties, a vertical transversely isotropic (VTI) model is chosen. A vertical transverse isotropic model represents materials that have the same properties in one plane and different properties in the normal direction. In this case, a horizontal plane, normal to the well, has the same properties while, vertically, the material shows different properties. To fully describe a vertical transverse isotropic material, 5 independent elastic constants are needed instead of the 2 independent variables required for an isotropic material or the 9 independent varabiables needed for orthotropic materials. The correspondent elastic constants are: E_h, E_v, v_h, v_v and G_{vh}. The compliance matrix takes the following form,

$$\begin{bmatrix}\varepsilon_{xx}\\ \varepsilon_{yy}\\ \varepsilon_{zz}\\ \varepsilon_{yz}\\ \varepsilon_{zx}\\ \varepsilon_{xy}\end{bmatrix} = \begin{bmatrix} 1/E_h & -v_{xy}/E_h & -v_{zx}/E_v & 0 & 0 & 0 \\ -v_{xy}/E_h & 1/E_h & -v_{zy}/E_v & 0 & 0 & 0 \\ v_{xz}/E_h & -v_{yz}/E_h & -1/E_v & 0 & 0 & 0 \\ 0 & 0 & 0 & 1/2G_{zx} & 0 & 0 \\ 0 & 0 & 0 & 0 & 1/2G_{zy} & 0 \\ 0 & 0 & 0 & 0 & 0 & 1+v_{xy}/E_h \end{bmatrix} \begin{bmatrix}\sigma_{xx}\\ \sigma_{yy}\\ \sigma_{zz}\\ \sigma_{yz}\\ \sigma_{zx}\\ \sigma_{xy}\end{bmatrix} \quad (3)$$

Two domains were built: A single crack domain containing only one rectangular crack located in the center and a domain with different ramifications whose purpose is to include natural cracks and a crack network.

The main objective to use these domains is to study the behavior of the fracture fluid and the resultant fracture geometry for a single crack and for a crack network.

Single crack domain will produce a long planar fracture with large width and high conductivity but with limited surface area. The complex fracture network will produce larger surface exposed area however risking to have craks with no conection to the main crack and hence unproductive.

Structural Model

Domains have a mesh of 3D elements representing the mass of rock sourrounding the crack and spring elements representing rock cohesive interface.

A geomechanical analysis of well stresses is carried out in an unfractured domain of the well to calibrate initial strains.

Information relevant to the model such as mechanical properties and *in situ* stresses are substracted from equations derived mainly from density and sonic logs, and calibrated with laboratory meassurements and field operations as DFITS and MFO. From sonic and density logs it is possible to calculate Poisson Ratio, Young's Modulus, Shear modulus, Bulk Modulus and Biot's coefficient; pore pressure can be taken as a normal trend or being calculated from different sorces such as sonic or resistivity logs. Vertical stresses are derivate from the depth and the density log, while maximum and minimum horizontal stresses are the result of the combination of such properties.

Since mechanical properties are available every few centimeters (approximately one foot), as shown in Fig.1, the data is stratified in order to insert them into the finite element mesh. The criterea adopted to consider that a new interval should be added considers rock elastic modulus and its variation along

well depth: When the Elastic modulus varies considerably in a relatively short length, then a new interval is created. The resultant model has ten different sets of rock properties as shown in Fig. 2a and Fig. 2b. Once the different intervals are stablished, mechanical properties are averaged for that specific interval but always preserving the anisotropic nature of the rock. This means that mechanical properties such as Young Modulus, Poisson's Ratio and subsecuently, Shear Modulus, and Biot's coefficient have horizontal and vertical components.

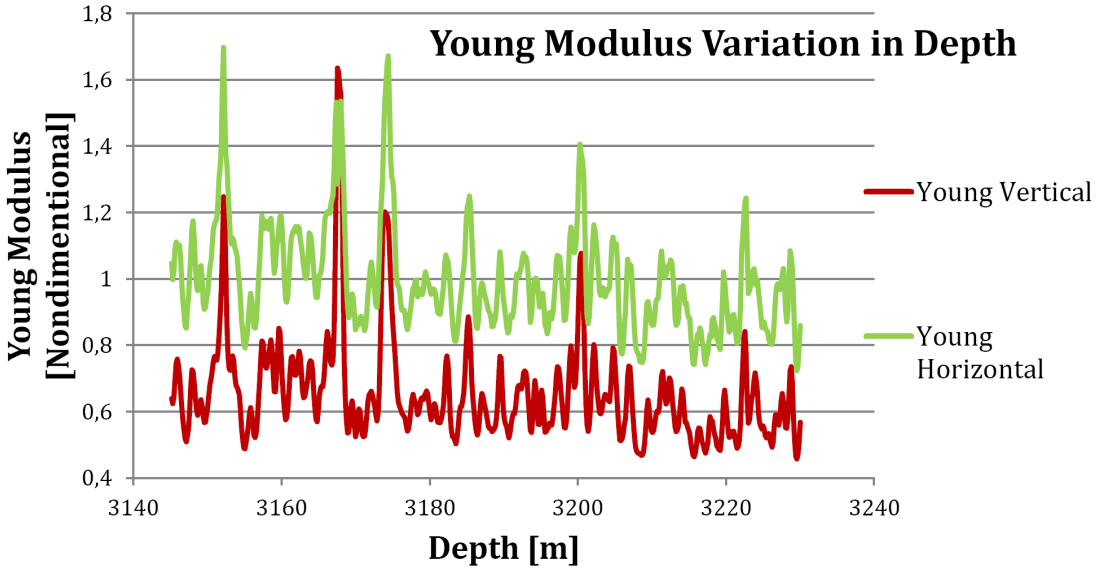

Figure 1—Horizontal and Vertical Young's Modulus as a function of depth. Values have been altered by dividing each value by the total average.

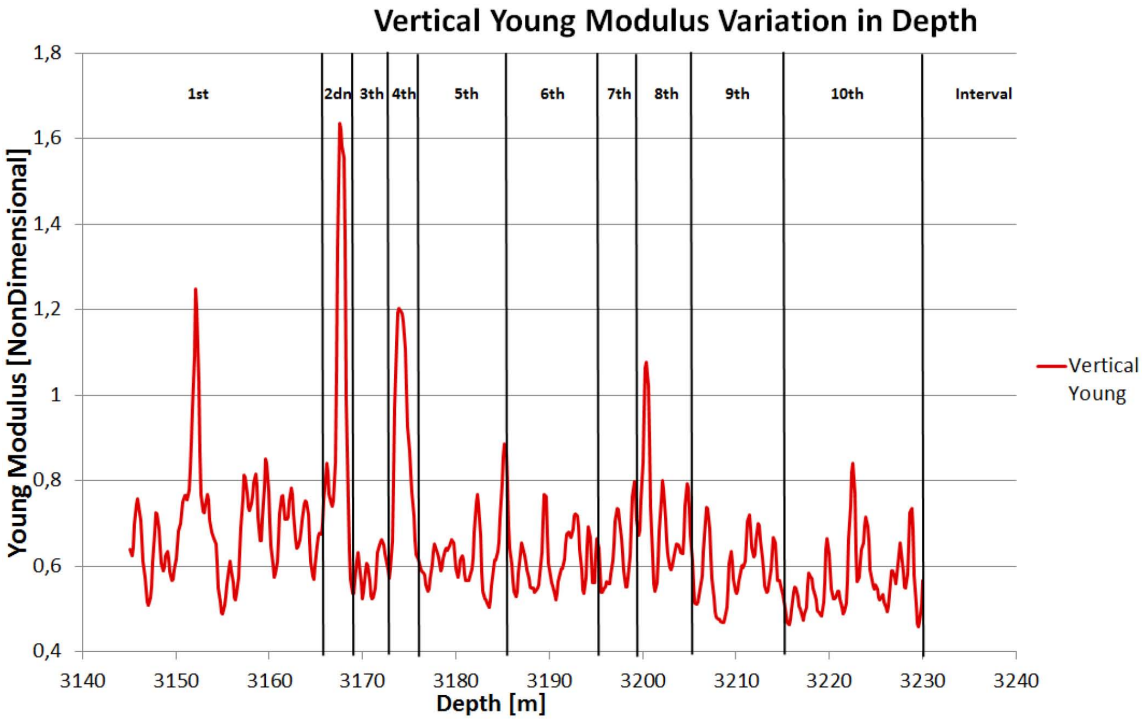

Figure 2a—Domain discretization addopted, in this example, considering 10 intervals. Vertical Young Modulus vs. Depth

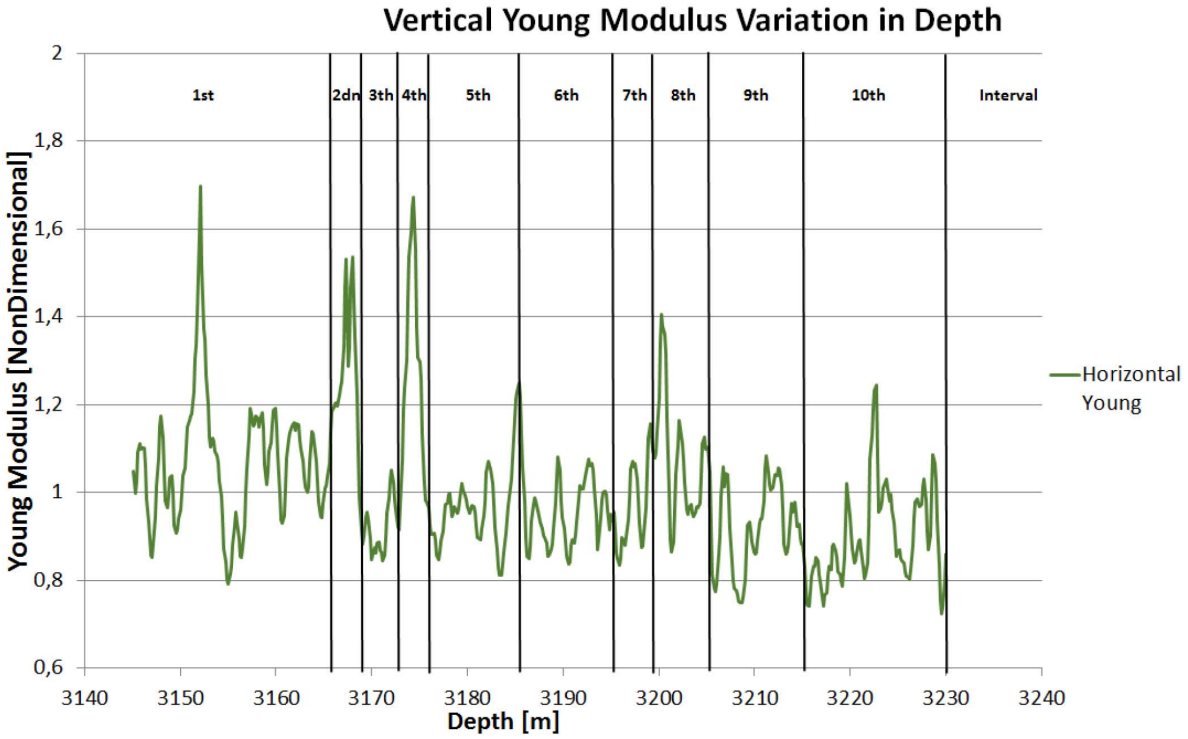

Figure 2b—Domain discretization addopted, in theis example, considering 10 intervals. Horizontal young modulus vs depth

This 10 intervals create a structural model of 90000 m^2 and 80 m depth with a imposed crack for injection fluid of 150×0.0508×30 m. The fracture's initial width is taken as 2 inches (50.8 milimeters) at the perforated casing. The structural model extension is set to have an appropriate size to display far field stresses as the tectonic and overburden loads to avoid nonuniform stress distribution around the fracture.

Regarding boundary conditions, a vertical symmetry plane parallel to the wellbore plane is used and a displacement restrictions applied at the bottom of the domain. In order to apply the horizontal and vertical stresses, since they vary considerably in function of depth, averaged principal stresses (minimum and maximum horizontal stress and vertical stress) and applied to domain faces as total loads.. In this way, load application is simplified considerably and changes in loads can be done easily. Pore pressure is applied as a load in the top and bottom faces of the model creating a vertical pore pressure gradient.

Load application is carried out in two stages: First stage consists of gradually loading the principal stresses to the model until *in situ* stresses, as calculated in the geomechanical analysis of the well, are reached. The second stage is the pumping schedule, consisting only of inyecting fracture fluid while the structural loads applied in the first stage remain constant.

To describe opening of the fracture, a cohesive model of damage is chosen by using non-linear springs located inside the fracture, in which every node in the fracture's boundary is joined with another node on the opoosite side of the fracture. A bilinear law relating relative displacement, between spring nodes, and the force done by the springs is used to represent rock's fracture toughness. This concept follows the formulation of cohesive zone model (CZM) developed by Barrenblatt (1959) and Dugdale (1960), that consist of a bilinear constitutive law relating traction and relative displacements and whose area represent Griffith's fracture energy. Since the parameters load opening law used in the models are forces instead of stresses, a simple arrangement is made for the nodes to integrate stresses into foreces depending on the element area. Springs are calibrated using mechanical properties such as Ultimate Compresive Strength (when spings are being compressed, meaning, relative displacements are negative) and Tensile Strength (when relative displacements are positive). During solution process, the fracture is considered opened once the spring has

reached the critical relative displacement for which the force is null. An example of the curve is shown in Fig.3. Relative displacements between nodes is calculated using the following equation,

$$U = (\boldsymbol{U^2} - \boldsymbol{U^1}).\frac{(\,{}^0x^2 - {}^0x^1)}{\|(\,{}^0x^2 - {}^0x^1)\|}, \tag{4}$$

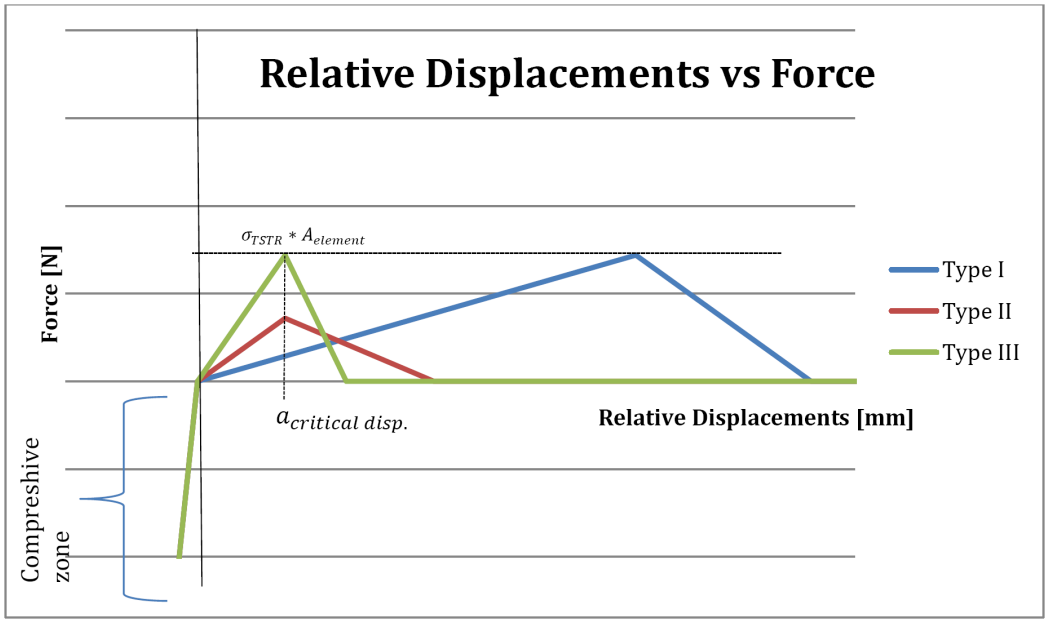

Figure 3—Example of the curves imposed to the non- lineal springs.

where ${}^0x^j$ is the initial position of the j node, and U^j is the correspondant displacement in the direction of the spring element.

Regarding nonlinear spring parameters, the most critical one is the relative displacement for which the force excert by the springs reaches its maximum, meaning, the fracture will expand. The definition of this paramenter was tailored with an analytical approach in order reproduce the magnitude of the aperture the spring will have to bear. Three different non-linear curves were adopted to account for different zones within the crack. Type I springs are placed at the beginning of the crack. Type II springs are located immediately after Type I springs and accounts for a semi-damage zone after punch operation. Therefore, a weaked element is used and that is the reason why only 50% of the Tensile Strength, σ_{TSTR}, of the rock is used. Type III springs are placed all along the crack where neither Type I nor Type II springs are placed, and accounts for a "no damaged zone". Once the order of magnitude of the critical displacement, $\alpha_{critical\ disp.}$ was established, three different curves were developed for the three types of non-linear springs.

To account for the porous media, permeability in each interval is considered. Porosity is not considered since fluid retained in pores is assumed to be water, with an incompressible behavior (at the present work). This leads to neglecting porosity effects but not the permeability. Another assumption done regarding porous media is that pores are fully saturated with pore fluid. This simplifies considerably the model. Hence, we get the following equation,

$$\nabla.\left(\boldsymbol{k}.\nabla P_f\right) = \frac{\partial \varepsilon_{ii}}{\partial t} + \frac{n}{\kappa_f}\frac{\partial P_f}{\partial t} \tag{5}$$

where $\boldsymbol{k}$ is the permeability matrix, ε_{ii} is the volumetric strain, n is the porosity and k_f is the bulk modulus of the porous fluid. When assuming the fluid is incompressible, k_f is sufficiently large to neglect the second term in the right side of the equation.

Fig.4 and Fig. 5 are images displaying the resultant models, single crack and multiple crack paths respectively, as seen from the software's user interfaces.

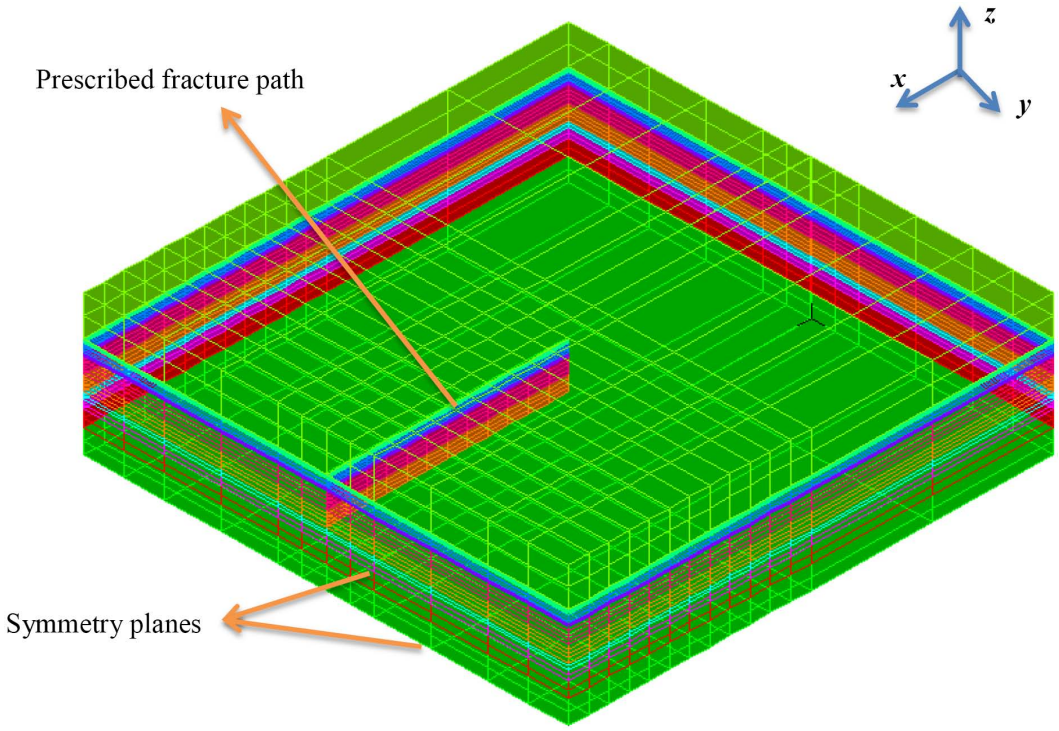

Figure 4—Domain showing the 10 different intervals (perceived as different colors) and the single rectangular cavity representing the fracture's path

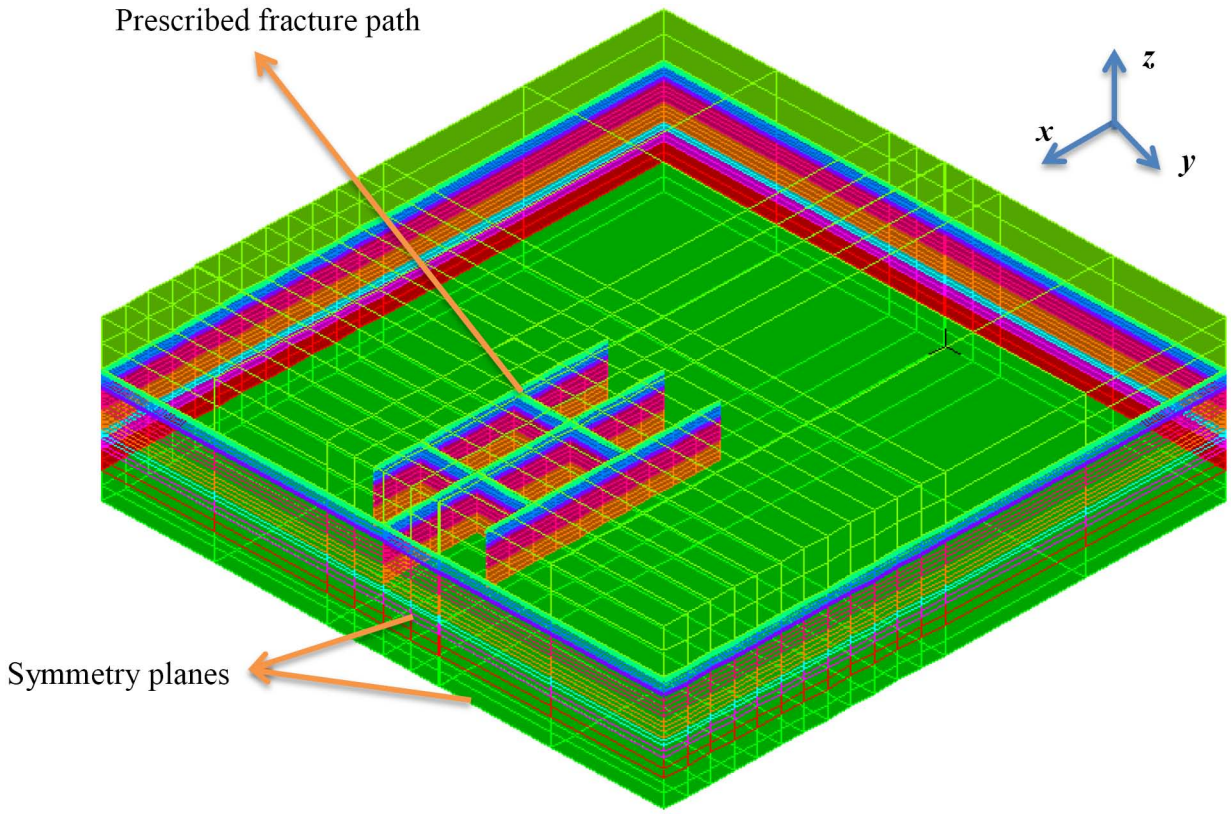

Figure 5—Domain showing the 10 different intervals (perceived as different colors) and the complex fracture network.

In Fig.5 as in Fig.6, symmetry planes are the "front" and bottom faces of the model. The rest of the faces are used to apply the corresponding forces. As mention, both models are 300×300×80 meters, while the fracture is 150×0.0508×30 meters.

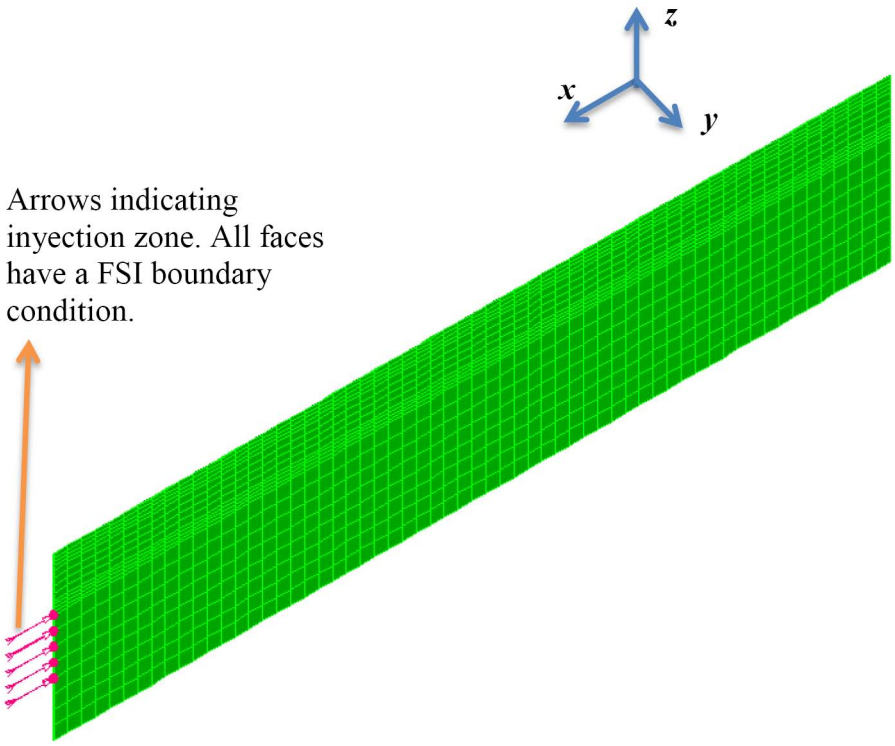

Figure 6—Fluid finite element model for a single crack.

Fluid Model

Fluid domain consists of a mesh of 3D-FCBI (Flow-Condition-Based-Interpolation) (K.J. Bathe and H. Zhang, 2002) elements with eight nodes for the injection fluid inside the crack rectangular cavity. For this model, pure water is used as injection fluid. Slightly compressible, Newtonian fluid and laminar flow between two permeable parallel plates is assumed. Since this problem includes a fluid domain enclosed by deformable boundaries, a slight compressibility is considered to increase stability. Flow- Condition-Based Interpolation elements, whose approach uses features from finite element and control volume methods to obtain discretization schemes that more effective. All variables are defined at corner nodes. These elements are highly recommended to be used in fluid structure interaction problems as consistent stiffness matrices are established for the complete fluid-structure system making it possible to solve complex practical problems with highly nonlinear responses. FCBI elements schemes are applicable to any Reynolds number flow.

Fluid properties are water properties and in this this model, only density, viscosity and bulk modulus are needed to fully describe the material properties. Properties remain constant for the entire solution.

The initial fracture geometry is exagerated to allow the fracture to growth freely and without any geometrical constraint. Fluid injection occurred at a specific depth selected considering rock's Young modulus, considered the most influential mechanical property that affects fracture's final geometry (Simonson, E.R., Abou-Sayed, A.S. and Clifton, R.J., 1978). Pumping schedule start as a lineal ramp going from 0 to 60 bpm in 60 seconds and after that it remains constant until a desired ammount of fluid has entered the domain.

Fig. 7 shows a visual of the model build in the single crack configuration while Fig.8 displays the fluid mesh for a complex crack network. Injection zone is marked in the figures with pink/red arrows. Fluid domain has the following dimensions: 150 meters in length, 50.8 milimeters in width and 30 meters high.

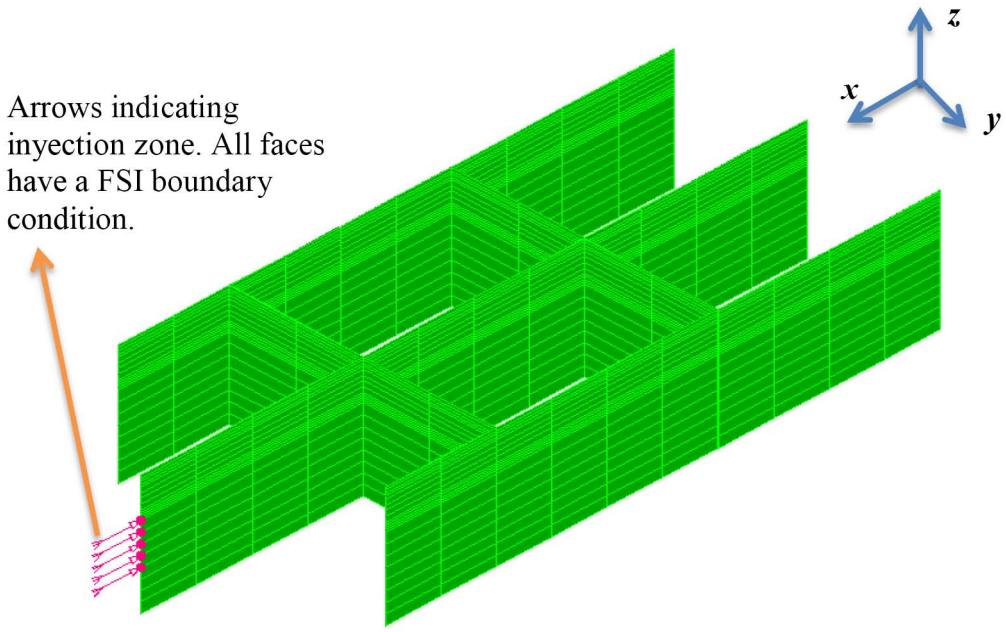

Figure 7—Fluid finite element model for the compex fracture network structural model.

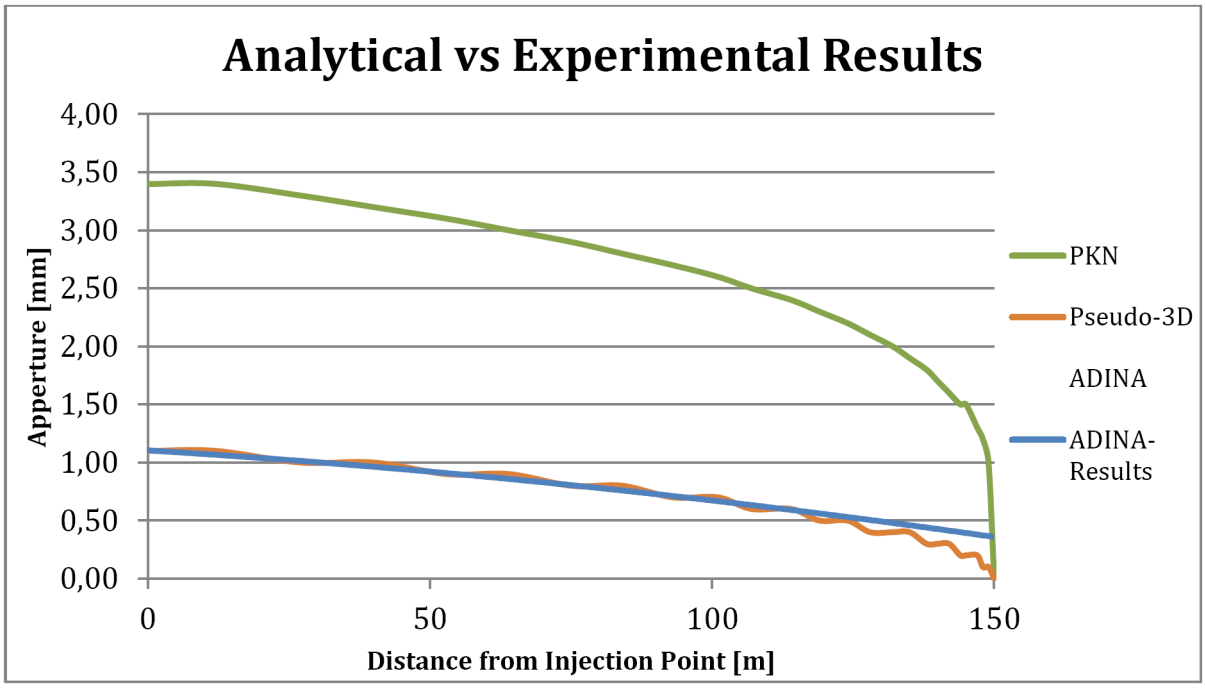

Figure 8—Graph showing fracture's width values along the fracture's length.

Results

Simple crack results

In order to compare the results obtained from the post processing simulation, analytical solution involving fracture geometry factors such as length, height and width are used. However, most of these equations demands assuming values of the fracture geometry that are completely unknown. Analytical solutions are obtained using Geertsma and Kern assumptions (J. Geertsma, and F. de Kern, 1969), which are:

- Planar fracture, meaning the fracture will propagate perpendicular to the minimum stress.

– Fluid flow is 1D
– Newtonian fluid
– Fracture completely confined in a single layer
– Rock assumed as a continiuous, homogeneous, isotropic linear elastic solid.

Hence,

$$w(x) = 3 \cdot \left[\frac{\mu\, q_i\, (L-x)}{E'}\right]^{1/4} \tag{6}$$

Equation (6)) relates fracture width as function of fracture's length, L, fluid flow, q_i, fluid's viscosity, μ, and the plain strain Young modulus, E ', that is calculated as

$$E' = \frac{E}{(1-v^2)} \tag{7}$$

where v is Poisson Ratio.

Equation (8)) states another way to calculate the resultant fracture's width considering rock's fracture toughness, K_{IC}, and the previously mention plane Young Modulus, E', this equation is used for planar pseudo 3D models:

$$w(x) = \frac{4\sqrt{2}\, K_{IC}}{\sqrt{\pi} * E'} \sqrt{x} \tag{8}$$

In Fig.8, it is possible to observe the solutions ploted in green and orange colors are the ones calculated using equation number 6 and 8, respectively. The blue line, with the legend ADINA, is the one obtained with the software. One can see the results approach considerably with the aperture calculated using equation 8. A very different solution is achieved by using equation 6 solution and higher values of fracture's width are obtained. This is definitely related with how each equation ponders Young's Modulus:PKN models has Young Modulus affected by the exponential ¼, while in Pseudo- 3D models it appears without any exponent. This is because of the different hypothesis handle on each model (Economides and Nolte, 2000).

The figure below (Fig. 9) shows perpendicular displacements to fracture's main direction (fracture's aperture). It is clear from the image that displacements vary not only in length but also in height. This is a direct consequence of rock's different mechanichal properties and high anisotrophy.

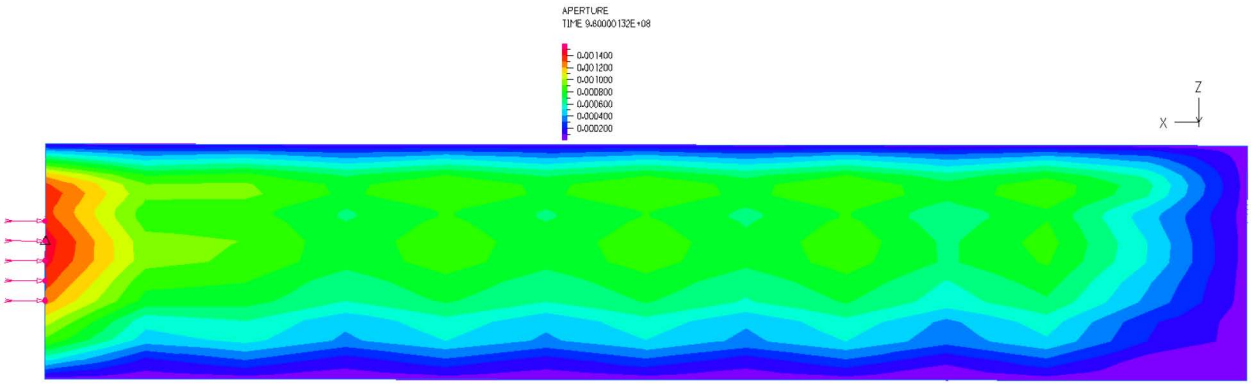

Figure 9—Fracture's resultant width. From the inyection point (left) to the fracture's full length. Results for single crack, as viewed from fluid model.

Figure 9 displays how a mayor aperture occurs in the zone near the injection point. When moving away from the injection zone, almost a constant and small value of aperture is register. Figure 9 also shows how appertures even near the injection zone varyies. This is mainly due to the different intervals applied to the

model and how each interval cointains different mechanical properties. More information about aperture values near the injection zone is shown in Table 1. The following figure, Fig. 10, displays aperture for a specific interval as shown in the structural model. In this image, injection zone is located to the right side of the image, which is why aperture values are higher at the right side.

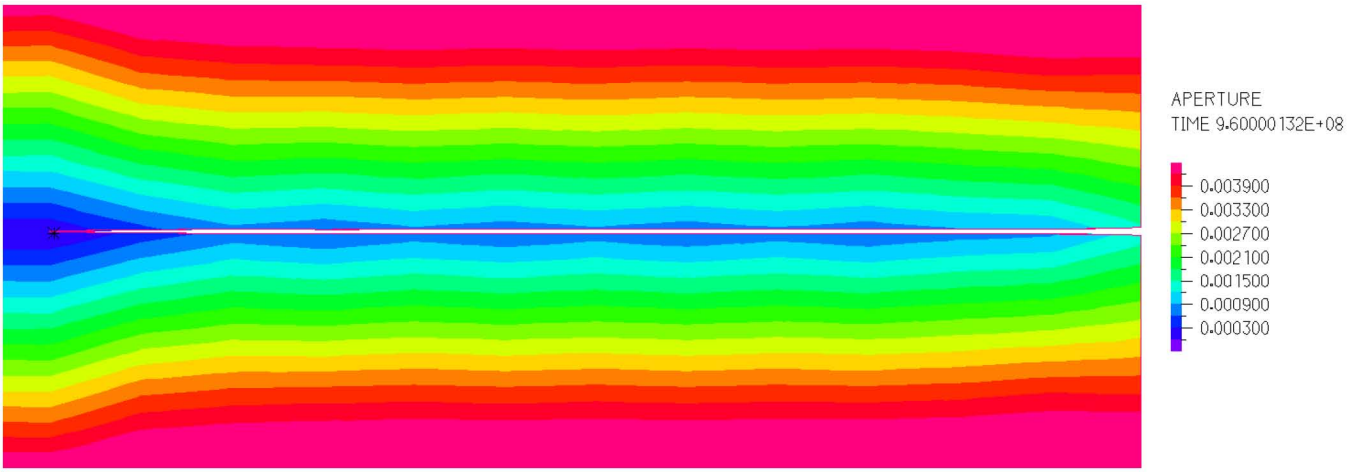

Figure 10—Fracture's aperture, top view, as seen from the structural model.

In the following table, maximum values of aperture are shown for each interval.

	Interval 1	Interval 2	Interval 3	Interval 4	Interval 5
ADINA Results	1.055 mm	1.4573mm	1.37166 mm	1.37862mm	0.85498 mm

The following figures are cross sections showing fracture's aperture in three different positions:

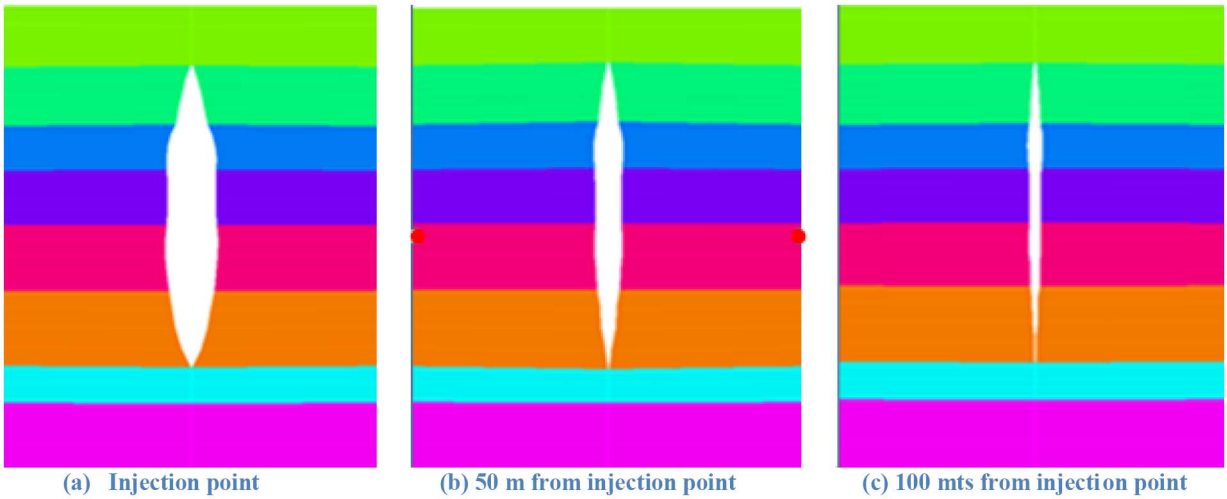

Figure 11—Cross sections displaying fracture's final geometry (displacements overmagnified).

Complex crack network results

Fig. 12 shows aperture values as seen from the fluid domain in the case of a multiple crack configuration. Higer values of aperture can be appreciated in the places where ramifications occur.

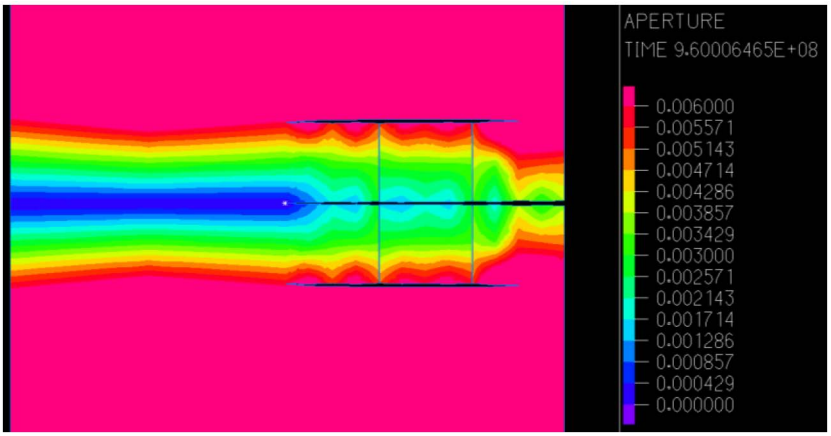

Figure 12—Aperture values in the complex fracture network model. Top view

Fig.13 is intended to display fluid movement inside the fracture. Injection zone is clearly visible on the right side of the image. After the first ramification, a significant amount of fluid is deviated from the central crack.

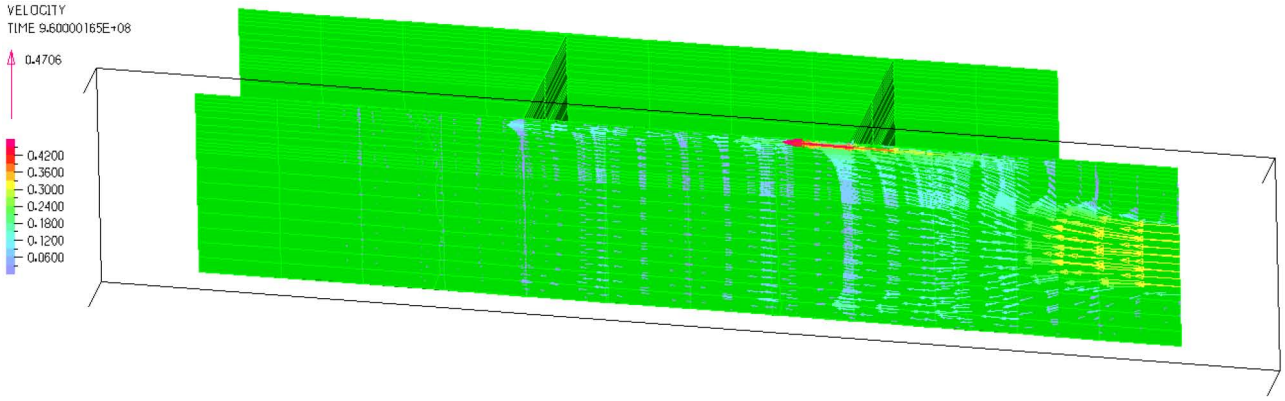

Figure 13—Velocity vectors in the fluid mesh. Image shows on half of the crack network.

Conclusions

The proposed model is a feasible option for simulating hydraulic fracture process when dominant cracks, even natural or generated, are present. Different well configurations in terms of porosity, permeability, formation's structure can be studied. Even under the same hypothesis, horizontal wells can be studied.

Carefull election of time step strategy is required to attain convergence along all the simulation stages. It is strongly dominated by rock mechanical properties and permeability. A larger time step must be considered when pore pressure in the whole domain is required. However, large time steps may cause convergence problems. On the other hand, working with short time steps and relatively big elements causes an irregular (zig-zag) pore pressure distribution near the fracture zone. By creating more elements however, it is expected to increase considerably computational effort.

Results for fracture's aperture in a single crack configuration have provide a good agreement with Pseudo 3D models.

Further development and convergence analysis is require in order to get the production curve after hydraulic fracture has been performed.

Acknowledgements

We would like to thank to the Center of Computational Mechanics and the Oil & Gas Laboratory in Buenos Aires Institute of Technology, PhD. Silvia Barredo and PhD. Eleonora Erdmann for their support and valuable experience and help during the process of this work.

References

1. Economides, M.J and Nolte, K.G. 2000. *Reservoir Stimulation*, third Edition, Texas: Wiley
2. Ertekin, T.; Abou-Kassem, J.H. and King, G.R. 2001. *Basic Applied Reservoir Simulation*, first Edition Vol. **7**, Richardson, Texas: SPE Textbook Series.
3. Economides, M.J; Oligney, R. and Valko, P. 2002. *Unified Fracture Design: Bridgin the gap between theory and practice*. First Edition. Alvin, Texas: Orsa Press.
4. Jaeger, J.C; Cook, N.G.W and Zimmerman, R.W. 2007. *Fundamentals of Rock Mechanics*, Fourth Edition, London: Wiley-Blackwell
5. Simonson, E.R.; Abou-Sayed, A.S. and Clifton, R.J., 1978, Containment of Massive Hydraulic Fractures,10.2118/6089-PA, *Society of Petroleum Engineers, SPE-6089-PA, SPE*.
6. Nordgren, R.P. 1972. Propagation of a Vertical Hydraulic Fracture. *Society of Petroleum Engineering Journal*, August, pp. 306–314.
7. Geertsma, J. and de Kern, F. 1969. *A Rapid Method of Predicting Width and Extend of Hydraulically Induced Fractures*. Society of Petroleum Engineers. 10.2118/2458-PA, Society of Petroleum Engineers, SPE-2458-PA, SPE.
8. Perkins, T.K.; Kern, L.R. 1961. *Widths of Hydraulic Fractures*. 10.2118/89-PA, Society of Petroleum Engineers, SPE-89-PA, SPE.
9. Mahrer, K. D. 1999. *A Review and Perspective on Far-Field Hydraulic Fracture Heometry Studies*.
10. Li, Q., Chen, M., Zhou, Y., Jin, Y., Wang, F. P., & Zhang, R. (2013, March 26). Rock Mechanical Properties of Shale Gas Reservoir and their Influences on Hydraulic Fracture. International Petroleum Technology Conference. doi:10.2523/IPTC-16580-MS
11. Soliman, Mohamed Y.; East, Loyd E.; Augustine, Jody R. 2010. *Fracturing Design aimed at Enhancing Fracture Complexity*,10.2118/130043-MS. Society of Petroleum Engineers. SPE-130043-MS. SPE
12. Soliman, M. Y., East, L. E., & Adams, D. L. 2008. *Geomechanics Aspects of Multiple Fracturing of Horizontal and Vertical Wells*. Society of Petroleum Engineers. doi:10.2118/86992-PA
13. Brenner, S. and Gudmundsson, A. 2004. *Arrest and aperture variation of hydrofractures in layered reservoirs*. Geological Society, London. doi:10.1144
14. Fisher, M. K., & Warpinski, N. R. 2011. *Hydraulic Fracture-Height Growth: Real Data*. Society of Petroleum Engineers. doi:10.2118/145949-MS
15. Cleary, M. P. 1978. Primary Factors Governing Hydraulic Fractures in Heterogeneous Stratified Porous Formations. Energy & Technology Conference of Petroleum Division, Houston, Texas, 5 November, 1978
16. Gupta, J. K., Albert, R. A., Zielonka, M. G., Yao, Y., Templeton-Barrett, E., Jackson, S. K., … Choi, N. H. 2013. *Integration of Fracture, Reservoir, and Geomechanics Modeling for Shale Gas Reservoir Development*. Society of Petroleum Engineers. doi:10.2118/164018-MS
17. Searles, K. H., Zielonka, M. G., Ning, J., Garzon, J. L., Kostov, N. M., Sanz, P. F., & Biediger, E. 2016. *Fully-Coupled 3D Hydraulic Fracture Models: Development, Validation, and Application to O&G Problems*. Society of Petroleum Engineers. doi:10.2118/179121-MS
18. Detournay, E., Adachi, J., Garagash, D. I. and Savitski, A. *Interpretation and Design of Hydraulic Fraturing Treatments*, United States Patent No. US 7111681B2, 2006.

19. *Adina User's Manual, Theory and Modeling Guide, Volume I: ADINA Solids & Structures*, ADINA R & D, Inc. Watertown, MA. 2016.
20. *Adina User's Manual, Theory and Modeling Guide, Volume III: CFD & FSI*, ADINA R & D, Inc. Watertown, MA. 2015.
21. Energy Information Administration, 2014. *Country Analysis note. United State*. http://www.eia.gov/todayinenergy/detail.php?id=14431
22. Mirzaei-Paiaman A, Dalvand K, Oraki-Kohshour I, Masihi M, Moghadasi J. 2012. "Formation damage: Aqueous phase trapping in shale and tight gas resources as a formation damage mechanism". *Energ Source Part A: Recovery, Utilization, and Environmental Effects* 2012; **34**(16): 1541–1549.
23. Casey, M., Rajan, S., Oraki Kohshour, I., Adejumo, A. T., & Kugler, I.2015. *"Assessment of shale resource development in Saudi Arabia and Middle East compared to North Americ"a* Society of Petroleum Engineers. doi:10.2118/172954-MS
24. Oraki Kohshour, I., Leshchyshyn, T., Munro, J., Yorro, M. C., Adejumo, A. T., Ahmed, U.,… Wedel, D. 2016. "Shale development face challenges in United States, especially in water as fracturing fluid". Unconventional Resources Technology Conference. doi:10.15530/URTEC-2016-2461040